Pair Momentum Distribution in $Bi_2Sr_2CaCu_2O_{8+\delta}$ Measured by Positron Annihilation: Existence and Nature of the Fermi Surface

L. P. Chan
Brookhaven National Laboratory, Upton, New York 11973

D. R. Harshman
AT&T Bell Laboratories, Murray Hill, New Jersey 07974

K. G. Lynn
Brookhaven National Laboratory, Upton, New York 11973

S. Massidda
Institut Romand de Recherche Numérique en Physique des Matériaux (IRRMA), PHB Ecublens, CH-105 Lausanne, Switzerland

D. B. Mitzi[(a)]
Department of Physics, Stanford University, Stanford, California 94305
(Received 22 February 1991)

We report the first measurement of the positron-electron momentum density in superconducting single-crystal $Bi_2Sr_2CaCu_2O_{8+\delta}$ ($T_c \approx 90$ K). The observed anisotropy exhibits a twofold (rather than fourfold) symmetry, which is attributed to the superlattice modulation along the b axis of the BiO_2 layers. Subtraction of the superlattice contribution also reveals a pair momentum distribution consistent with the CuO_2 and BiO_2 Fermi surfaces, and in reasonable agreement with the theoretical pair momentum density derived from band theory.

PACS numbers: 73.20.At, 74.70.Vy, 78.70.Bj

Several theoretical models have been posited, ranging from a simple renormalized Fermi-liquid picture [1] to the more exotic anyon-field theories [2], in an effort to understand the nature of the pairing mechanism behind high-T_c superconductivity. Although each of these models can provide a plausible picture, their validity is ultimately subject to the actual electronic structure and properties of the material. Of particular relevance to this issue is the existence and nature of the Fermi surface. Given this, it is not surprising that a great deal of experimental effort has been expended on understanding the normal-state electronic properties of the CuO_2-based materials, with particular emphasis being given to angle-resolved photoemission spectroscopy and positron two-dimensional angular correlation of annihilation radiation (2D-ACAR) [3]. Indeed, recent photoemission studies [4] in $Bi_2Sr_2CaCu_2O_{8+\delta}$ have reported effects consistent with a Fermi surface, and in reasonable agreement with band-structure calculations [5,6]. In this contribution, we present the first 2D-ACAR study of the $Bi_2Sr_2CaCu_2O_{8+\delta}$ system, showing the Fermi surface associated with the CuO_2 layers and providing evidence for the existence of a BiO_2 electron pocket near the M point.

The 2D-ACAR technique is described elsewhere [7], so only a short discussion will be given here. Briefly, one measures the projection, $N_z(p_x,p_y)$, of the pair (e^-e^+) momentum density, where $\hat{\mathbf{z}}$ is normally chosen to be along a principal crystallographic direction. In the limit of the independent-particle approximation, and assuming zero temperature, $N_z(p_x,p_y)$ can be written as

$$N_z(p_x,p_y)=\int dp_z\,\rho^{2\gamma}(\mathbf{p})=\text{const}\times\int dp_z\sum_{j,\mathbf{k}}n_j(\mathbf{k})\left|\int d\mathbf{r}\,\psi_+(\mathbf{r})\psi_{j,\mathbf{k}}(\mathbf{r})e^{i\mathbf{p}\cdot\mathbf{r}}\right|^2$$
$$=\text{const}\times\int dp_z\sum_{j,\mathbf{k}}n_j(\mathbf{k})\sum_{\mathbf{G}}|A_j(\mathbf{k},\mathbf{G})|^2\delta(\mathbf{p}-\mathbf{k}-\mathbf{G})\,, \tag{1}$$

where the A_j's are the Fourier coefficients of the thermalized e^+ ($k^+=0$) and e^- (k,j band index) Bloch wave products $\psi_+\psi_{j,\mathbf{k}}$, the $\mathbf{G}$'s are the reciprocal-lattice vectors, and $n_j(\mathbf{k})$ is the electron occupation number of the jth band. Thus, under ideal conditions, i.e., in the absence of complications arising from defects and positron wave-function effects, a Fermi surface (if it exists) would be manifested as discontinuities in $N_z(p_x,p_y)$. To suppress core and valence contributions, $N_z(p_x,p_y)$ is folded into the first Brillouin zone using the Lock-Crisp-West (LCW) technique [8], resulting in the reduced momentum distribution,

$$\tilde{N}_z(p_x,p_y)=\text{const}\times\int dp_z\sum_{\mathbf{k},\mathbf{G},j}n_j(\mathbf{k})\delta(\mathbf{p}-\mathbf{k}-\mathbf{G})\times\sum_{\mathbf{G}'}|A_j(\mathbf{k},\mathbf{G}')|^2\,, \tag{2}$$

where $\mathbf{k}$ is restricted to the first zone. In the limit that the coefficients $A_j(\mathbf{k},\mathbf{G}')$ are $\mathbf{k}$ independent, the reduced momentum distribution is proportional to the occupation number $n_j(\mathbf{k})$, whose discontinuities represent the Fermi

surface.

The measurements were performed on a single crystal of unannealed material having exact cation stoichiometry, $Bi_{2.1}Sr_{1.94}Ca_{0.88}Cu_{2.07}O_{8+\delta}$ (with ± 0.03 stoichiometric error), and a superconducting transition temperature of $T_c \approx 90$ K. The crystal, dimensioned $20\times10\times0.1$ mm^3, was grown by a directional solidification technique described elsewhere [9]. The face-centered orthorhombic (quasitetragonal) unit cell has lattice parameters $a = 5.413 \pm 0.002$ Å, $b = 5.411 \pm 0.002$ Å, and $c = 30.89 \pm 0.01$ Å, and an incommensurate superlattice modulation along the b direction with $\mathbf{q} = \mathbf{b}^*/4.7$ (where $b^* = 2\pi/b$) [10,11]. The experiments were conducted in vacuum ($< 10^{-6}$ Torr), with the crystalline c axis oriented to within $\pm 2°$ along $\mathbf{z}$ (i.e., the integration direction), thereby allowing direct observation of the pair momentum density in the a-b plane. The two annihilation gammas were detected using two Anger cameras [7], each positioned a distance of 15 m (along $\hat{\mathbf{z}}$) on either side of the sample. A coincidence count rate of 20 counts/s was obtained with a resolving time of 5.0 ± 0.2 μs. The resulting experimental resolution was found to be 0.5 mrad FWHM. The data were centered with an accuracy of $\sigma = \pm 0.03$ channel (0.004 mrad) and corrected using a momentum sampling function [7]. Data were taken at 40, 110, and 295 K, with accumulated events totaling 85×10^6, 25×10^6, and 21×10^6, respectively. Utilizing the quasitetragonal character of the crystal structure, a reduced χ^2 method [12] was employed where the deviation of the counts at corresponding symmetric positions about both the a and b axes were minimized to establish the crystal orientation in the a-b plane.

Theoretical calculations (assuming a face-centered orthorhombic structure) of the e^-e^+ momentum density were performed within the framework of the local-density approximation, using the electronic band-structure results obtained earlier [5], with the full-potential linearized augmented-plane-wave method [13]. The positron ground-state wave function was obtained by adding an e^-e^+ correlation energy to the inverted crystal Coulomb potential [14]. Annihilation enhancement was also included according to Ref. [15]. About 1×10^3 vectors were used to fold $\rho^{2\gamma}(\mathbf{p})$ according to the LCW procedure [8].

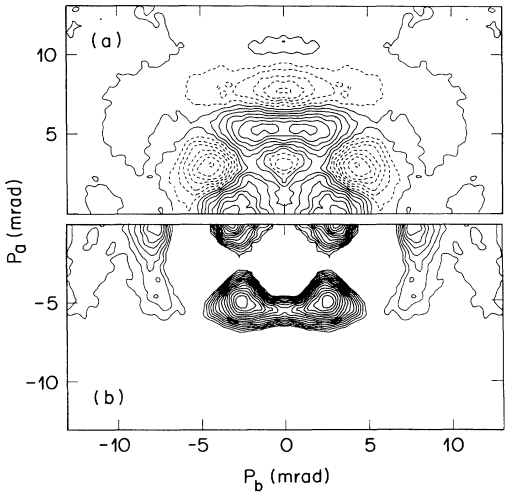

FIG. 1. (a) The anisotropy at 40 K, obtained from subtracting the radius-averaged isotropic function from the corresponding parent spectrum. (b) The residual spectrum at 40 K, obtained by subtracting the fourfold construction spectrum from the corresponding parent spectrum. P_a and P_b represent the momenta along the a and b axes, respectively.

For the p_z integration, the single-band contributions to the reduced momentum density, $\tilde{\rho}^{2\gamma}(\mathbf{p})$, as well as the corresponding one-electron energies, were interpolated (in an extended zone scheme) with a smooth Fourier series [16]. The interpolated values on 64 p_z planes in the first Brillouin zone (combined with a Fermi factor) were used to obtain the $\tilde{N}_z(p_x,p_y)$ distribution.

To examine the small anisotropies, a "radius-averaging" manipulation was performed, whereby a smooth angular average (constructed from the mean number of counts at each momentum radius) was subtracted from each of the three spectra. Owing to the quasitetragonal unit cell, we expected a fourfold symmetric anisotropy. Interestingly, however, the resulting (unsymmetrized) anisotropies for all three temperatures were instead found to exhibit twofold symmetry [17], which we attribute to the incommensurate modulation along the b axis [10,11]. The effect of the b-axis modulation can be represented as an additional term in Eq. (1), namely,

$$n_z^m(p_x,p_y) = \text{const} \times \int dp_z \sum_{j,k} n_j(\mathbf{k}) \sum_{\mathbf{G}} |A_j(\mathbf{k},\mathbf{G},\mathbf{q})|^2 \delta(\mathbf{p}-\mathbf{k}-\mathbf{G}\pm n\mathbf{q}) , \quad (3)$$

where $n\mathbf{q}$ is the modulation vector parallel to $\mathbf{b}^*$ (n is an integer). In this case, the signals are translated by $\pm\mathbf{q}$, and modulated by the $\mathbf{q}$-dependence Fourier coefficients of the e^-e^+ pairs in the BiO_2 layers. Further support for this assignment comes from theoretical calculations [18], indicating the positron wave function in $Bi_2Sr_2CaCu_2O_8$ to be preferentially distributed along the BiO_2 layers. Note that the positron density distribution used in the present work agrees well with that of Ref. [18]. In order to preserve the twofold symmetry, the three spectra were each symmetrized about the a and b axes, smoothed using a Gaussian with a FWHM equal to the experimental resolution (0.5 mrad), and volume normalized. We denote the resulting symmetrized, smoothed, and normalized data as "parent" spectra. A section of anisotropy extracted from the 40-K parent spectra is shown in Fig. 1(a), where the solid and dotted curves correspond to counts above and below the symmetric construction, respectively. The 110- and 295-K anisotropies were found to exhibit similar features, each showing an anisotropy of

$(2.0 \pm 0.3)\%$.

The existence of the incommensurate modulation along the b axis is problematic, since the Brillouin zone is not well defined. To circumvent this, we have developed a method of generating a fourfold symmetric distribution by transforming the parent spectra in a manner which suppresses the lower-symmetry components. Denoting the number of events (of the 40-K parent spectra) at position (p_i,p_j) by $N(p_i,p_j)$, we define

$$\begin{aligned} N_{ij} &= N(p_i,p_j) = N(-p_i,p_j) \\ &= N(p_i,-p_j) = N(-p_i,-p_j)\,, \\ N_{ji} &= N(p_j,p_i) = N(-p_j,p_i) \\ &= N(p_j,-p_i) = N(-p_j,-p_i)\,. \end{aligned} \tag{4}$$

Thus, to impose fourfold symmetry under which these eight positions are equivalent, we apply the transformation

$$N'(\pm p_i,\pm p_j) = N'(\pm p_j,\pm p_i) = \min[N_{ij},N_{ji}]\,, \tag{5}$$

where the positive and negative signs are independently permuted. Figure 1(b) shows a section of the residual anisotropy obtained by subtracting the fourfold symmetric distribution [constructed using Eqs. (4) and (5)] from the 40-K parent spectrum. Continuing on the premise that the superlattice induces a twofold perturbation, the features exhibited in the residual spectrum simply reflect the modulation component of the momentum distribution.

The anisotropy derived from radius averaging the fourfold symmetric construction and that of the full theoretical momentum density are $(1.2 \pm 0.1)\%$ and 3.2%, respectively. As a consequence, a valid comparison can only be made by considering the experimental and theoretical anisotropies. The first derivatives of cuts along ΓX (or equivalently ΓY) through either the experimental or theoretical anisotropies yield no clear signatures of the CuO_2 band crossings. The absence of strong effects along ΓX and ΓY is not surprising, however, since the Cu $d_{x^2-y^2}$ component of $\psi_{j,k}(\mathbf{r})$ is an odd function of $\mathbf{r}$, such that the integral along the ΓX and ΓY symmetry lines is identically zero. Thus, we do not expect to observe strong features arising from the CuO_2 bands in the spectrum. Figure 2 shows the cuts along ΓM of the fourfold experimental and theoretical anisotropies. While the agreement with theory is certainly reasonable, the data within the first zone (zone boundary located 3.2 mrad from Γ) exhibit a broadening, possibly attributable to remnant superlattice modulation [19] along ΓM. Outside the first zone the first derivatives of the 40 K and theoretical anisotropies show minima at 3.6 and 4.0, respectively.

In the case of LCW folding [8], the resulting distribution along k_x (and k_y) includes contributions from umklapp terms with $G_x \neq 0$ (and $G_y \neq 0$), which are nonzero because of broken symmetry in the exponential term of Eq. (1). The CuO_2 signatures still appear weakest along the symmetry lines, ΓX and ΓY, where the sum of the two CuO_2 Fermi-surface contributions to the LCW is 10 times smaller than that from the (unoccupied) BiO_2 band. As one moves away from these symmetry lines toward the M point, however, the CuO_2 contribution becomes 4 times greater than that of the BiO_2 band. Near the M point, the hybridization of the CuO_2 and BiO_2 bands near E_F (see Ref. [5]) produces an additional enhancement of the CuO_2 contribution to the LCW. Positron wave-function effects are also present, away from the Fermi-level crossings and near Γ and toward X and Y. Figure 3 shows cuts and associated first derivatives along ΓM and ΓX of the fourfold experimental and theoretical LCW spectra. The cut along ΓM [Fig. 3(a)] through the theoretical LCW distribution indicates a peak at 3.2 mrad, with the associated first derivative exhibiting a peak at 2.5 mrad (associated with the BiO_2 band crossing) as well as a shoulder (arising from the CuO_2 hybrid-

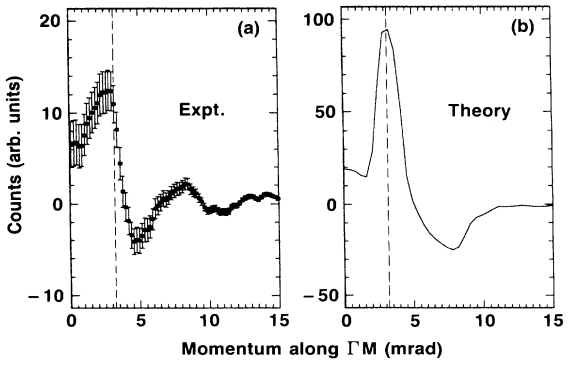

FIG. 2. Cuts along ΓM through the (a) 40-K fourfold experimental anisotropy and (b) theoretical momentum density. The zone boundary is 3.2 mrad from Γ.

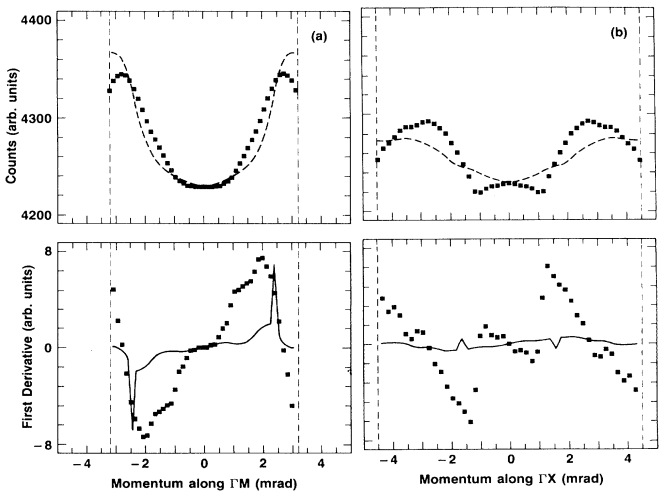

FIG. 3. The cuts and associated first derivatives along (a) ΓM and (b) ΓX of the experimental fourfold LCW. The dashed and solid curves correspond to the convoluted (with our experimental resolution) and unconvoluted theoretical LCW.

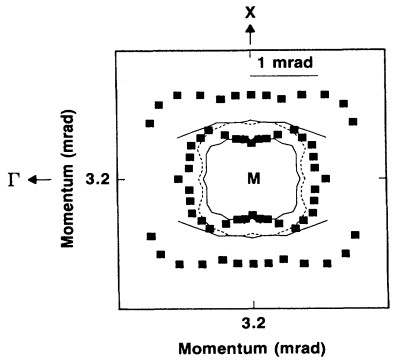

FIG. 4. The BiO_2 and CuO_2 Fermi surfaces near the M point, represented by the locus of the extrema in the first derivatives of various cuts through the M point. The solid symbols correspond to the 40-K LCW spectrum, the solid curve to the unconvoluted full theoretical spectrum, and the dashed curve to the convoluted (with our experimental resolution) full theoretical spectrum.

ization with the BiO_2 band) beginning at ~ 1.3 and ending at ~ 2.3 mrad. Comparison with our 40-K fourfold spectrum shows qualitative agreement, but with slightly different k-space positions; the peak in the cut occurs at 2.9 mrad, while the peak and shoulder of the first derivative occur at about 2 and ~ 1 (extending to 1.7) mrad, respectively. Along ΓX [Fig. 3(b)], the first derivative of the 40-K fourfold spectrum yields a break at 1.4 mrad, which is consistent (within experimental error) with the 1.6 mrad estimated from our momentum density calculation. Contrary to calculations, however, the data exhibit maxima rather than minima along ΓX. Fortunately, this seemingly inconsistent result can be resolved by considering the size of the positron wave-function effects along ΓX, which appear to be larger than that predicted by our theory. Figure 4 shows the loci of extrema in the first derivative of various cuts through the M point of our fourfold LCW spectrum. A comparison with theory is also shown, where the solid and dashed curves represent the loci of extrema in the first derivatives of similar cuts through the unconvoluted and convoluted (with our experimental resolution) theoretical LCW spectra, respectively. If we interpret the experimental data in Fig. 4 as band crossings, then the closed surface around the M point would be consistent with the BiO_2 electron pocket, and the remaining outer two surfaces with the CuO_2 Fermi surfaces. Our data would further imply that there exists a much wider separation between the BiO_2 and CuO_2 Fermi surfaces than predicted by current theory. Cuts along XMY lend further support to this conclusion [20], and suggest a possible photoemission study along XMY.

In summary, we have measured the e^+e^- pair momentum distribution in $Bi_2Sr_2CaCu_2O_{8+\delta}$ using positron 2D-ACAR, and compared these results with theory. The experimental data supported the presence of a BiO_2 Fermi surface about the M point, as predicted by band theory. There is also evidence of Fermi breaks associated with the CuO_2 band crossings along ΓX and possibly near M, although exhibiting a comparatively weaker signature owing to symmetry considerations and the small overlap of $\psi_+(\mathbf{r})$ with the CuO_2 planes. Near the M point, our results (if interpreted in terms of band crossings) indicate a greater separation between the BiO_2 and CuO_2 Fermi surfaces than predicted by band theory. We also observe temperature-dependent fine structure in the anisotropy, exhibiting effects opposite to thermal broadening, in agreement with others [21].

We are grateful to J. H. Kaiser and R. N. West for providing the LCW program, S. Berko for his early involvement in instrumentation, and A. J. Freeman and J. Yu for their collaboration on the electronic structure calculation. We also thank M. Schlüter, W. E. Pickett, D. Singh, M. Peter, and co-workers for insightful discussions, and P. Mijnarends *et al.* for a preprint of their work. This work is supported in part by the U.S. Department of Energy under Contract No. DE-AC02-76CH-00016. Work at IRRMA is supported by the Swiss National Foundation under Contract No. 20-5446.87.

[a]Present address: IBM T. J. Watson Research Center, Yorktown Heights, NY 10598.

[1] D. M. Newns *et al.*, Phys. Rev. B **38**, 6513 (1988); D. M. Newns *et al.*, Phys. Rev. B **38**, 7033 (1988); J. H. Kim *et al.*, Phys. Rev. B **39**, 11633 (1989).
[2] Y. H. Chen *et al.*, Int. J. Mod. Phys. B **3**, 1001 (1989).
[3] For a recent review of the state of the field see, Conference Proceedings of the Workshop on Fermiology of High-T_c Superconductors, Argonne National Laboratory, 25–27 March 1991 [J. Phys. Chem. Solids (to be published)].
[4] C. G. Olson *et al.*, Phys. Rev. B **42**, 381 (1990); B. O. Wells *et al.*, Phys. Rev. Lett. **65**, 3056 (1990).
[5] S. Massidda *et al.*, Physica C **152**, 251 (1988).
[6] M. S. Hybertsen and L. F. Mattheiss, Phys. Rev. Lett. **60**, 1661 (1988); H. Krakauer and W. E. Pickett, Phys. Rev. Lett. **60**, 1665 (1988).
[7] R. N. West *et al.*, J. Phys. E **14**, 478 (1981).
[8] D. G. Lock, V. H. C. Crisp, and R. N. West, J. Phys. F **3**, 561 (1973).
[9] D. B. Mitzi *et al.*, Phys. Rev. B **41**, 6564 (1990).
[10] S. A. Sunshine *et al.*, Phys. Rev. B **38**, 893 (1988); Y. Gao *et al.*, Science **241**, 954 (1988).
[11] C. H. Chen *et al.*, Phys. Rev. B **37**, 9834 (1988).
[12] L. C. Smedskjaer and D. G. Legnini, Nucl. Instrum. Methods Phys. Res., Sect. A **292**, 487 (1990).
[13] H. J. F. Jansen and A. J. Freeman, Phys. Rev. B **30**, 561 (1984).
[14] E. Boronski and R. K. Nieminen, Phys. Rev. B **34**, 3820 (1986).
[15] T. Jarlborg and A. K. Singh, Phys. Rev. B **36**, 4660 (1987).
[16] D. D. Koelling and J. H. Wood, J. Comput. Phys. **67**, 253 (1986).
[17] L. P. Chan *et al.*, Bull. Am. Phys. Soc. **35**, 483 (1990).
[18] D. Singh *et al.*, Phys. Rev. B **39**, 9667 (1989).
[19] J. Friedel and M. Peter, Europhys. Lett. **8**, 79 (1989).
[20] L. P. Chan *et al.*, in Ref. [3].
[21] P. E. Mijnarends *et al.*, Physica C **176**, 113 (1991); in Ref. [3].